EXPERIMENTAL DATA ON AN ADVANCED SOLAR-POWERED ADSORPTION REFRIGERATOR

F. Buchter[1], C. Hildbrand[1], Ph. Dind[1], and M. Pons[2]

[1] Laboratoire d'Énergétique Solaire, EIVD (HES-SO), 1, Route de Cheseaux, CH-1400 Yverdon-les-Bains, Switzerland
[2] C.N.R.S.-L.I.M.S.I., B.P. 133, F-91403 Orsay Cedex, France

ABSTRACT

An adsorptive solar refrigerator was built and tested in September 2000 in Yverdon-les-Bains, Switzerland. The adsorption pair is silicagel + water. The machine does not contain any moving part, it does not consume any mechanical energy except for experimental purposes and it is relatively easy to manufacture. The adsorber is a solar collector at the same time (flat-plate, 2 m^2, double glazed), the condenser is air-cooled (natural convection) and the evaporator contains 38 litres of water that can freeze into ice. This ice is a cold storage for the cabinet (320 litres). Elements such as valves and a graduated bottle are installed only for experimental purposes. Experimental measurements are presented and analysed. Performances of the machine are very promising with a gross solar cooling COP near 0.19. This value is higher than the ones obtained by former solar-powered refrigerators (0.10-0.12) despite some restrictive effects in the evaporation connected with the use of water as refrigerant and cold storage. Moreover, an energy balance of the solar collector shows that the collector efficiency (0.41) is greater than the values (0.3-0.35) reported in former experiments.

RESUME

Un réfrigérateur solaire à adsorption fut construit et testé durant le mois de septembre 2000 à Yverdon-les-Bains en Suisse. Le couple d'adsorption utilisé est : gel de silice + eau. Le système ne possède aucune pièce en mouvement, ne consomme pas d'énergie mécanique (excepté pour les mesures expérimentales) et est relativement simple de conception. Le système est composé d'un collecteur solaire (capteur plan de 2 m^2, avec double-vitrage) faisant office d'adsorbeur, d'un condenseur à air (convection naturelle) et d'un évaporateur contenant 38 litres d'eau, eau susceptible de geler à l'intérieur de l'évaporateur. Cette glace est un stock de froid pour l'enceinte frigorifique (320 litres). Des vannes et un réservoir gradué sont installés pour l'expérimentation. Les données expérimentales sont présentées et analysées. Les performances du système sont très prometteuses, avec un COP solaire brut atteignant 0,19. Cette valeur est supérieure à celles atteintes par d'autres systèmes de réfrigération solaire (0,10-0,12), ceci en dépit des contraintes liées à la prise en glace de l'eau à l'intérieur de l'évaporateur. De plus, un bilan énergétique du capteur solaire montre que le rendement de captation (0,41) est supérieur aux valeurs (0,3-0,35) obtenues par de précédentes expérimentations.

KEYWORDS

Solar energy, silicagel, water, adsorption, cooling, experiment, double glazed flat-plate solar collector.

- - - -

1. INTRODUCTION

The concept of using solar energy for powering a refrigerator arose forty years ago [1] with a prototype using a liquid sorption cycle. Solar-powered refrigeration can also use solid sorption, either chemical reaction [2-4] or adsorption. Meunier has published a comparison of those three sorption systems for solar cooling [5]. The solid-gas system used in the present study is adsorption.

Several groups have tested solar cooling with adsorption. Among reported experimental machines, some of them use sophisticated solar collectors with concentration [6-8] but the most efficient configuration seems to consist of metallic flat-plate solar collectors, single- or double-glazed, covered with selective surface and filled with the adsorbent itself [9-20].

All the machines reported in the articles [6-20], either with chemical reaction or with adsorption, follow an alternative cycle heating/cooling, also said 'intermittent', the period of which corresponds to the alternation day/night. Moreover, as they do not require any additional source of energy, those machines are completely autonomous and therefore appropriate to be used in remote areas.

Considering performance, the highest values of COP (0.10-0.12) were obtained with the adsorption systems zeolite + water [14] and activated carbon + methanol [10, 11, 17]. If methanol can easily evaporate at temperatures below 0°C, thus favouring the production of ice, water surely is the most environment-friendly refrigerant. With water, ice can be produced *within* the evaporator, acting as a 'cold storage'. Both refrigerants, water or methanol, operate at under-atmospheric pressure and therefore require vacuum technology.

The main purpose of the present study is to obtain, with a technically speaking simple machine, better performances than the ones reported above. This aim seems reasonably achievable with an adsorptive

machine, operated in a 100% solar-powered 24-hour cycle with flat-plate, solar collectors containing the adsorbent. However, when referring to the works reported above, both the efficiency of the solar collector and that of the adsorption thermodynamic cycle may be improved. These requirements lead to the design of the 'advanced' machine.

2. DESCRIPTION OF ADSORPTION

Adsorption, alias physisorption, is the process by which molecules of a fluid are fixed on the walls of a solid material. The adsorbed molecules undergo no chemical reaction, they simply lose energy when being fixed: adsorption, the phase change from fluid to adsorbate (adsorbed phase) is exothermic. Moreover it is reversible. In the following, we will focus on adsorption systems mainly used in cooling (or heat-pumping) machines: a pure refrigerant vapour that can easily be condensed at ambient temperature and a microporous adsorbent with a large adsorption capacity.

The adsorption equilibrium of a one-component fluid is bivariant: the thermodynamic state of the system is defined by two quantities, e.g. the temperature of the solid phase, T, and the pressure of the refrigerant vapour, P. Prescribing these two quantities gives, among other features, the amount of adsorbate fixed in the micropores, ε. The vapour pressure P is lower than the saturation pressure of the liquid-vapour equilibrium at the same temperature, $P_s(T)$. The adsorption equilibrium is such that when the temperature T is increased, or when the pressure P is decreased, the adsorbed amount ε decreases. As a consequence, an alternation of heating/cooling periods makes the adsorbent pump out and in the vapour, like a thermally driven piston. This is the basis of the adsorption cooling cycle.

3. PRINCIPLE OF THE ADSORPTION COOLING CYCLE

The main components of an adsorptive cooling machine are the adsorber (in the present case, the solar collector itself), the condenser, the evaporator and a throttling valve between the two latter devices, see Figure 1. An ideal cycle is presented in the Dühring diagram (LnP vs. $-1/T$), Figure 2. The cycle is commented on in the following paragraphs at the same time as the operation of the solar refrigerator is described (4 steps).

3.1. Step 1: Isosteric heating

At sunrise, the collector-adsorber is at low temperature T_i, slightly higher than ambient temperature at this moment, and the vapour pressure is (ideally) the one fixed by the evaporator temperature: $P = P_e = P_s(T_e)$, see point A in Figure 2. The collector-adsorber is disconnected from the evaporator, e.g. by closing the check valve (see (6) in Figure 1). If ventilation dampers are installed (see (2) in Figure 1), they are shut (position (2a)) for reducing the heat losses of the collector. The solar heating makes the temperature of the collector-adsorber increase. As the connection with the evaporator is closed, the vapour phase is superheated and its pressure can increase without any condensation nor desorption. As a consequence, the system follows an isosteric path (i.e. with constant adsorbed amount), see AB in Figure 2. During this step, the system is pressurised.

When the vapour pressure reaches the value of the saturation pressure at the condenser temperature, i.e. when $P = P_c = P_s(T_c)$, see Point B in Figure 2, condensation can occur. This point is usually reached between 9 and 11 a.m., depending on the irradiance.

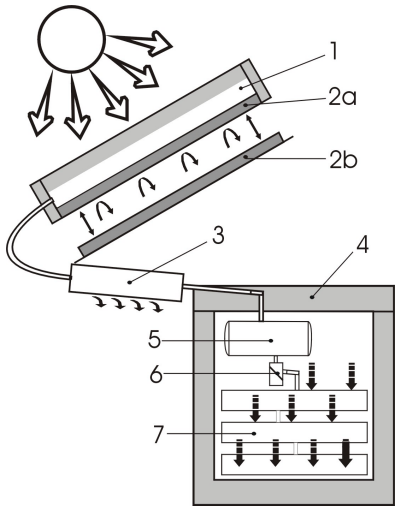

Figure 1: Scheme of an adsorptive solar refrigerator: solar collector-adsorber (1), ventilation dampers (2) closed (2a) and open (2b), condenser (3), cold cabinet (4), graduated bottle (5), check valve (6), evaporator and ice storage (7).

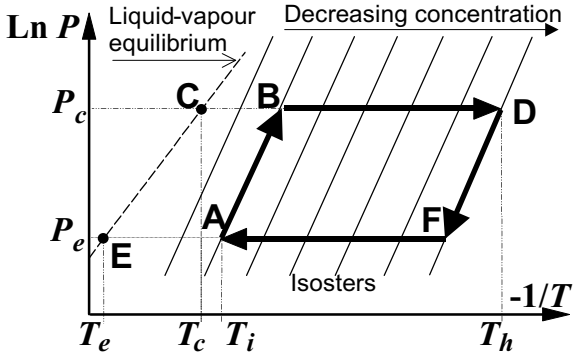

Figure 2: An ideal adsorption cooling cycle in the Dühring diagram. Saturation liquid-vapour curve for the refrigerant (EC dashed line), isoster curves (thin lines), adsorption cycle (thick lines). Heating period: step AB (7. a.m. – 10. a.m.) and step BD (10. a.m. – 4. p.m.); cooling period: step DF (4. p.m. – 7. p.m.) and step FA (7. p.m. – 7. a.m.).

3.2. Step 2: Desorption and condensation

Once point B is reached, the condenser temperature (ideally constant) fixes the pressure in the system and any increase in the adsorbent temperature results in desorption, see the path BD in Figure 2, ideally isobaric (see point C in figure 2). The refrigerant vapour desorbed from the collector-adsorber is cooled and liquefied in the condenser, which consequently releases heat to ambient air. The liquid refrigerant at T_c is collected in a graduated bottle for measurement, see (5) in Figure 1.
As long as the solar heat supply is larger than the heat losses of the collector-adsorber, the temperature of the latter increases, which adds more to the amount of 'processed' (i.e. desorbed and condensed) refrigerant. However, after noon the solar irradiance decreases with time, while the heat losses of the collector increase with its temperature. Eventually a time comes when the collector-adsorber reaches its maximal temperature, denoted as T_h. This moment corresponds to point D in Figure 2, usually reached between 3 and 5 p.m. At that moment, the entire liquid refrigerant is transferred from the graduated bottle into the evaporator (see (7) in Figure 1), which is afterward kept disconnected from the adsorber until step 4.

3.3. Step 3: Isosteric cooling

After that moment, the temperature of the collector-adsorber cannot do anything else but decrease: the cooling period of the cycle begins. The decrease in the adsorber temperature can be favoured when ventilation dampers are installed on the units. Opening these dampers (position (2b) in Figure 1) allows ambient air, moved by natural convection, to flow along the collector and thus to cool it more efficiently than conduction only through insulation. The temperature decrease of the adsorber induces a pressure decrease in isosteric conditions. At that stage (path DF in Figure 2), the system is depressurised.
When pressure reaches the value of the saturation pressure at the evaporator temperature, $P = P_s(T_e)$, see Point F in Figure 2, the valve (see (6) in Figure 1) closed in the morning for disconnecting the evaporator from the adsorber, is now open, allowing the refrigerant to evaporate. This usually occurs between 4 and 6 p.m.

3.4. Step 4: Adsorption and evaporation

The temperature of the evaporator, ideally constant, now fixes the pressure. The temperature of the adsorbent continues decreasing: vapour is adsorbed and consequently pumped from the evaporator into the adsorber, see in Figure 2 the path FA, ideally isobaric. The refrigerant, transferred as liquid into the evaporator at the end of step 2, evaporates and extracts heat at low temperature from the cold cabinet. When, like presently, the evaporator contains more water than processed by the cycle, the freezing of this water fixes the evaporation temperature at 0°C.

This period corresponds to the night. At sunrise, the temperature of the collector-adsorber is minimal, the system has reached point A and the cycle is closed.

4. DESCRIPTION OF THE MACHINE TESTED IN YVERDON-LES-BAINS, SWITZERLAND

4.1. General features

In order to obtain better COP than the values reported in ref. [10, 11, 17], both the efficiency of the solar collector and that of the thermodynamic cycle must be improved. This leads to the selection of a collector-type, concentrating or flat-plate, together with the selection of an adsorption pair.
First of all, for ecological reasons, the refrigerant is water, which leads to two possible adsorption pairs: zeolite + water or silicagel + water. It is well known that the first pair yields good COP when the desorption temperature is rather high (150-200°C) while the second pair is most often used when the desorption temperature lies around 100°C. As a result zeolite would be used with a low-concentration collector (e.g. Compound Parabolic Collector) and silicagel with an efficient flat-plate collector (e.g. double glazed or transparent insulation materials). A rapid preliminary study has shown that the configuration silicagel with double glazed collector, when correctly designed, offers a good compromise between performance and complexity of the machine. The adsorbent is then a microporous silicagel (*Actigel SG®, Silgelac*).

4.2. Collector-adsorber

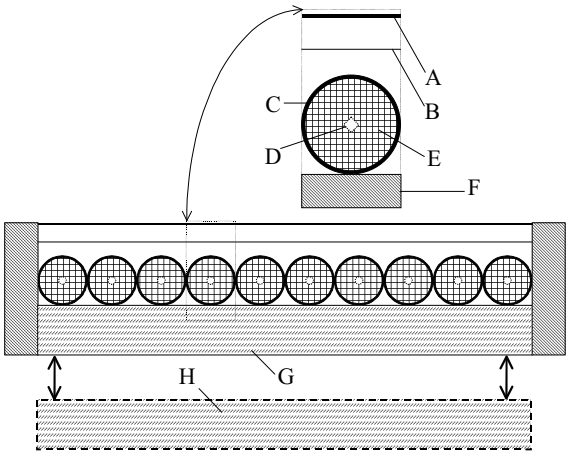

Figure 3: Scheme of the solar collector-adsorber: glass cover (A), teflon film (B), tube covered with selective surface (C) and internally layered with Papyex®, central tube for vapour transport (D), silicagel bed (E), thermal insulation around the collector (F); insulating dampers are also shown in closed position (G) and open position for ventilation (H).

The solar collector (2 m^2, tilt angle of 30°) is double-glazed: a Teflon film is installed between the glass and the adsorber itself. This film reduces the convective and radiative heat losses between the adsorber and glass cover. The adsorber consists of 12 parallel tubes (72.5 mm in diameter) that contain the silicagel (78.8 kg). The tubes are covered with an electrolytic selective layer (Chrome-black, *Energie Solaire SA*), which absorbs 95% of the visible solar radiation while presenting an emissivity of 0.07 in the infrared wave-lengths. In order to improve the thermal conductivity of the silicagel bed, the tubes are layered with a material of good conductivity but low specific heat capacity (sheets of graphite: *Papyex®, Le Carbone Lorraine*). A central tube made out of a grid (diameter 15 mm, mesh 1 mm, wire 0.45 mm diameter) allows the water vapour to flow easily along the tube. Figure 3 presents a scheme of the collector as well as a detail of the tubes. The ventilation dampers mentioned in the previous sections consist of a mechanism that allows to 'open' the thermal insulation on the rear side of the collector (50 mm glass wool) as shown in Figure 3, to provide efficient cooling by natural convection during the night.

4.3. Condenser

Eight parallel finned tubes make a condenser, cooled by natural convection of air. The pitch between fins is 12 mm. The total fin area is of 6.9 m^2, which should guarantee a temperature difference with ambient lower than 10 K.

4.4. Evaporator, ice storage and cold cabinet

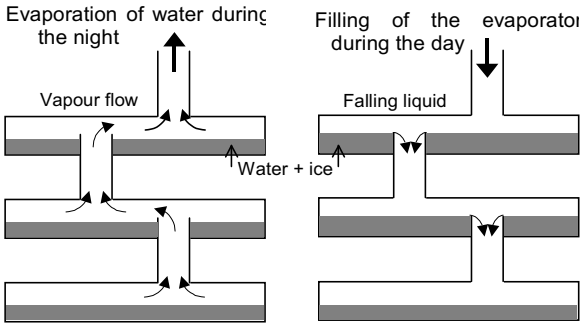

Figure 4: Scheme of the evaporator and representation of water flows during evaporation (night) and during filling (mid-afternoon).

The evaporator consists of three rings made with square tubes arranged as shown in Figure 4. The total heat exchange area is 3.7 m^2. The evaporator can contain 38 litres of water. During evaporation, part of this water turns into ice, which acts as a 'cold storage' so that the cold chamber is kept cold, not only until the next night but also for a period of three days of low irradiation, assuming a thermal load of 27 litres water at 20°C introduced each day.

The cold cabinet is of the chest-type. Well insulated (170 mm of expanded polystyrene), its internal available volume is of 320 litres.

4.5. Valves and instrumentation

In the present configuration, a valve is needed on this machine, the one located between the graduated bottle and the evaporator. The other valves have been implemented for experimental purposes only.
Temperature is measured (platinum probes Pt100) in the collector-adsorber, on three condenser tubes and three evaporator tubes; ambient air temperature is also measured. Vapour pressure is measured in the condenser (piezo gauge 0-25 kPa) and in the evaporator (piezo gauge 0-10 kPa). Global irradiance in the plan of the collector is recorded by a pyranometer (*Kipp-Zonen*).
A graduated bottle (7.3 litres) collects the condensed water, see (5) in Figure 1. The level of liquid water is read on graduations, more or less regularly during the desorption step.
Apart from the level of liquid water, all the measurements are automatically recorded every 10 seconds. Moreover, the ventilation dampers and the valve opening and closing times are recorded.

5. TYPICAL EXPERIMENTAL RESULTS

Figures 5, 6 and 7 show typical measurements obtained on a rather sunny day. The four steps of the cycle as well as the points A, B, D, and F, mentioned in Figure 2 can be recognised. These figures can be commented as follows.

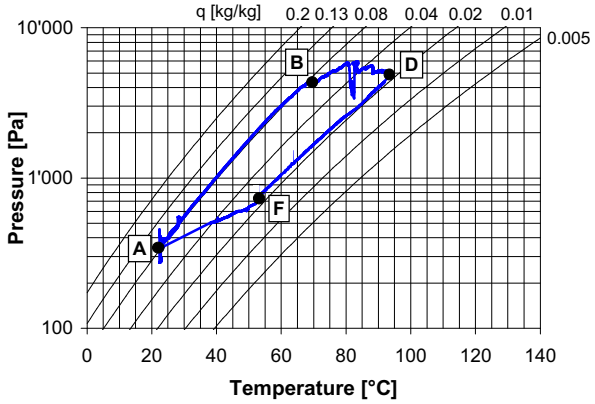

Figure 5: Presentation of the experimental cycle in the Dühring diagram for 13th September, 2000. The effects of the blocking of evaporation can be readily seen. Apart from this point, the experimental cycle is rather close to the ideal cycle shown in Figure 2.

Due to irradiance variations, ambient temperature and condensed flow-rate (and therefore in the thermal power-rate released by the condenser), desorption does not perform at constant pressure like in the ideal cycle shown in Figure 2.

The effect of a cloudy period (between 11.30 a.m. and 1. p.m.) on the adsorbent temperature and vapour pressure can be readily seen, while its effect on the amount of condensed water is hardly noticeable. This is due to the cumulative principle of the solid-sorption cooling cycle.
The temperature difference between condenser and ambient air is always less than 10 K.

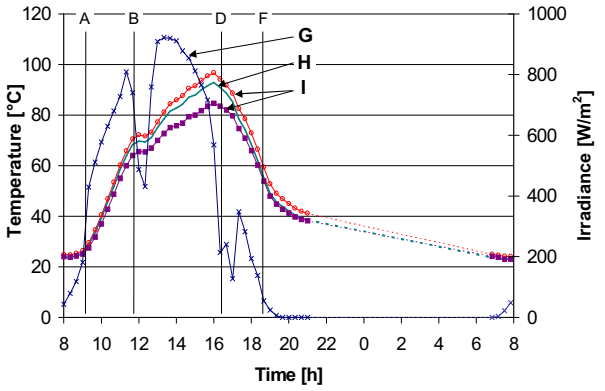

Figure 6: Typical measurements over a day/night period. Temperatures (I) and average temperature (H) of collector-adsorber and irradiance (G), (13th September, 2000).

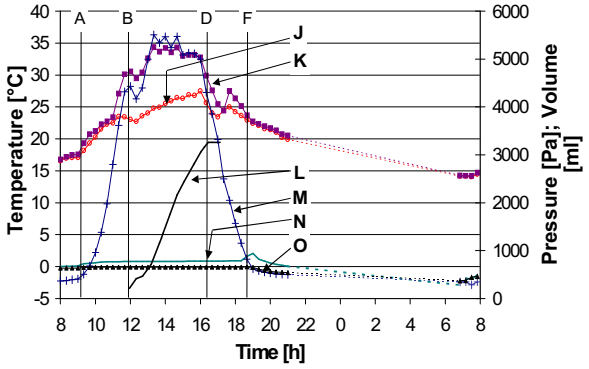

Figure 7: Typical measurements over a day/night period. Temperature of condenser (K), evaporator (N) and ambient air (J); vapour pressure in condenser (M) and evaporator (O); volume of processed water (L) (13th September, 2000).

The temperature in the cold cabinet remains in the range [+2, +4°C]. A load is introduced every day during the measured period in order to simulate a real use of the refrigerator. The temperature of the evaporator remains below 1°C all day long and drops down to –3°C during the night. This behaviour means that evaporation of water is replaced by sublimation of ice, although a quantity of water in the evaporator is still liquid. In other words, a small quantity of ice actually creates a thin layer between the water and the vapour. By sublimation, the temperature of this small amount of ice drops down below 0°C, while the liquid water remaining in the evaporator is at a temperature slightly higher than 0°C. This behaviour is inherent in using water as refrigerant and cold storage at temperatures near 0°C. However a better design of the evaporator can reduce this effect. This point is to be mentioned because it can readily be understood that such a behaviour (sublimation instead of evaporation) reduces the experimental performance of the machine.

6. PERFORMANCE OF THE TESTED UNIT

For each day, a gross solar COP_{SR} can be defined as the ratio of the heat extracted by evaporation of water to the solar heat supply, see equation 1. The first one, Q_e, is obtained by multiplying the mass of processed water, m_L, by the enthalpy difference between the saturated vapour at T_e and the saturated liquid at T_c. The second one, Q_h, is the product of the surface S of collector and the solar irradiation obtained by integrating the solar irradiance G from sunrise to sunset. This yields the following expression for the gross solar COP_{SR}:

$$COP_{SR} = \frac{Q_e}{Q_h} = \frac{m_L \cdot [L - Cp_L \cdot (T_c - T_e)]}{S_{fs} \cdot \int_{\text{sunrise}}^{\text{sunset}} G(t).\mathrm{d}t} \qquad (1)$$

On 13th September, 2000, the solar heat supply for the 2 m^2 collector, Q_h, was 41.7 MJ. The amount of processed water was 3.26 litres, which corresponds to a gross heat extraction, Q_e, of 7.8 MJ. As a result, the gross solar COP_{SR} is 0.19.
This value of COP_{SR} is excellent (about 50% higher than the ones previously published) and can be commented as follows. First of all, the ambient temperature was rather low (between 15 and 25°C, see Figure 7) which is very favourable to the cycle efficiency. Secondly, the solar irradiation was fair but not very large: it often happens that it raises up to 25 MJ.m^{-2} or more. Thirdly, as already mentioned, some ice sublimation occurred in the evaporator. As a result, the evaporation pressure at the end of the night lied around 400 Pa (see Figure 7) instead of the usual 600 Pa with water as refrigerant. This dramatic reduction of pressure (-33%) significantly reduces performance. As a conclusion, when gathering these three arguments, it can be expected that a similar machine yields COP_{SR} approaching 0.2, even in an African climate.
When the heat losses of the refrigerated chest (actually the heat input from ambient, evaluated at 1.3 MJ for that day) are subtracted from the heat extraction, one obtains the net heat extraction and the net solar COP_{SN}, which is of 0.16 for that day.

7. ENERGY BALANCE OF THE SOLAR COLLECTOR

The energy balance of the solar collector is established with the help of all the temperatures measured in the adsorber. The heat balance involves different temperature gradients (in the cross-section of the tubes, along their length and between the different tubes). This balance permits to evaluate on the one hand the

different losses of the collector and on the other hand the collected energy, Q_{coll}. The Sankey diagram, Figure 8, summarises the heat balance.

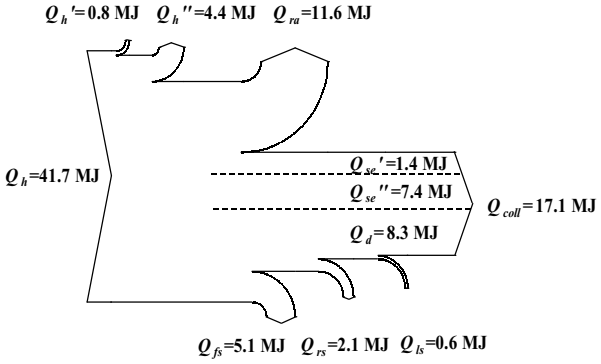

Figure 8: Distribution of the different heat quantities involved in the heat balance of the collector-adsorber for 13th September, 2000, with: Q_h = Solar heat supply (sunset to sunrise); Q_h' = Solar heat supply before the beginning of heating; Q_h'' = Solar heat supply after the end of desorption; Q_{ra} = Losses by reflection and absorption of the doubled-glass; Q_{se}' = Sensible heat of the inert; Q_{se}'' = Sensible heat of the silicagel and the water (included in the silicagel); Q_d = Heat of desorption; Q_{coll} = Collected energy; Q_{fs} = Losses front side; Q_{rs} = Losses rear side; Q_{ls} = Losses lateral side.

Collector losses are composed of several parts: unused irradiation before the beginning of heating and after the end of desorption, losses due to reflection and absorption of visible wavelengths by the double glazing, infrared and conductive-convective losses on the front side of the collector, and conductive-convective losses on its other sides.
The losses due to reflection and absorption of visible wavelengths by the double glazing take into account the angle of incidence of direct solar radiation on the collector. The effective absorptance of the double-glazing-cover adsorber system $(\tau\alpha)_{eff}$ has been calculated on the basis of the equations found in [21] and [22]. Finally, one obtains these losses by applying the following equation :

$$Q_{ra} = S_{fs} \cdot \int_{t_A}^{t_D} G(t) \cdot (1 - (\tau\alpha)_{eff}) \cdot dt \qquad (2)$$

This energy (Q_{ra}) is evaluated to be 11.6 MJ.
The losses of the collector-adsorber are separated in three parts: losses of the front side, of the rear side and of the lateral sides. The first one takes into consideration the conductive, convective and radiative heat transfers between the different layers (tube-Teflon film, Teflon film-glass and glass-ambient). The general equation used for this determination is:

$$Q_{fs} = S_{fs} \cdot \int_{t_A}^{t_D} h_{fs}(t) \cdot (T_t - T_a) \cdot dt \qquad (3)$$

with coefficient h_{fs} defined by :

$$h_{fs}^{-1} = \frac{1}{h_{cv,tf} + h_{cc,tf} + h_{r,tf}} + \frac{1}{h_{cv,fg} + h_{cc,fg} + h_{r,fg}} + \frac{1}{h_{cv,ga} + h_{r,ga}} \qquad (4)$$

The different coefficients of this equation are calculated according to the theory of heat transfer. The numerical result of Q_{fs} is 5.1 MJ.
The losses by the lateral side and by the rear face include the conductive heat transfer through the sides of the collector and the convective heat transfer to the surroundings. The radiative heat transfer of these surfaces is disregarded because of the low emissivity of the aluminium coating of the collector. The losses are defined according to:

$$Q_{rs,ls} = S_{rs} \cdot \int_{t_A}^{t_D} h_{rs}(t) \cdot (T_t - T_a) \cdot dt + S_{ls} \cdot \int_{t_A}^{t_D} h_{ls}(t) \cdot (T_t - T_a) \cdot dt \qquad (5)$$

with h_{rs} and h_{ls} defined according to:

$$h_{rs} = \frac{1}{\frac{1}{h_{cv,rs-a}} + \frac{1}{h_{cc,rs-a}}} \qquad (6)$$

$$h_{ls} = \frac{1}{\frac{1}{h_{cv,ls-a}} + \frac{1}{h_{cc,ls-a}}} \qquad (7)$$

Q_{rs} is 2.1 MJ and Q_{ls} 0.6 MJ.

The collected energy useful for the cycle divides into three terms: the sensible energy for heating the inert elements (tubes, dampers and *Papyex*®), the sensible energy for heating the silicagel and the water it contain, and the energy of desorption. In order to take into account the temperature gradients along and across the tubes, they have been divided into several sections. The sensible energy is defined for each section *j* by:

$$Q_{se,j} = \sum_{X=st,pa,sg,w} m_X \cdot Cp_X \cdot (T_{X,tD} - T_{X,tA}) \qquad (8)$$

The total energy Q_{se} is given by the sum $\Sigma Q_{se,j}$, which yields to 1.4 MJ for the inert and 7.4 MJ for the silicagel + water.
The quantity of water contained in the silicagel is defined by the equation of Langmuir:

$$\varepsilon = q_s \cdot \frac{(b \cdot P)^n}{1 + (b \cdot P)^n} \qquad (9)$$

with:

q_s	= 0.544	[kg.kg^{-1}];
b	$= b_0 \cdot exp\left(\frac{-\Delta H_0}{R \cdot T}\right)$	[Pa^{-1}]
b_0	= 3.186.10^{-12}	[Pa^{-1}]
ΔH_0	= -2.637.10^{6}	[J.kg^{-1}]
n	= 1.3	[-]

The energy of desorption is calculated for each section by mean of the following equation:

$$Q_{d,j} = m_{sg} \cdot \int_{t_A}^{t_D} \Delta H \cdot (\varepsilon_{(t+1)} - \varepsilon_{(t)}) \cdot dt \qquad (10)$$

The total energy Q_d, which results in 8.3 MJ, is the sum of the energies of the different sections.
With these figures, the collected energy, Q_{coll}, is evaluated at 17.1 MJ. It results that the collector efficiency, η, defined as: $\eta = \frac{Q_{coll}}{Q_h}$, reaches the value of 0.41. This is significantly larger than the values of 0.3-0.35 published in earlier performed experiments [14, 17]. It is worth noticing that the main contribution to the heat losses is due to reflection of the solar irradiation and its absorption by the double glazing. This significant heat loss (28% of the solar heat supply) is the counterpart of the very strong reduction of the infrared and conductive-convective losses. Indeed, these two heat losses are only 12% of the solar heat supply.

The ratio of the heat extraction (gross or net) by the collected energy yields the COP of the adsorption cycle itself. The obtained values are: COP_{CR} = 0.46 (gross) and COP_{CN} = 0.38 (net). Again, these values are higher than the ones formerly published for solar experiments: 0.38 (gross) with the zeolite + water pair [14] or 0.43 (gross) -0.32 (net)- with the active carbon + methanol pair [18]. It finally appears that the improvement in performance obtained with this new solar-powered adsorption refrigerator is partly due to the double glazing and partly due to the selection of the silicagel + water pair.

8. CONCLUSION

Provided a consistent design of the collector-adsorber was applied, the combination of a double-glazed flat-plate solar collector covered by an efficient selective surface with the adsorption pair silicagel + water and improving the conductivity of the silicagel bed permits to obtain solar cooling COP_{SR} around 0.19, i.e. significantly greater than the ones previously obtained. Such performance of solar-powered autonomous cooling machines might open new markets, especially with the present desires to save energy and reduce global warming.

Acknowledgements

The "Fonds stratégique of the University of Applied Sciences of Western Switzerland (HES-SO)" and "l'Ambassade de France à Berne" are gratefully acknowledged for their financial support.

REFERENCES

[1] Chinnappa J.C.V., Performance of an intermittent refrigerator operated by a flat-plate collector, *Solar Energy*, **Vol. 6**, pp. 143-150, 1962.

[2] Worsøe-Schmidt P., Solar refrigeration for developing countries using a solid absorption cycle, *Int. J. Ambient Energy*, **Vol. 4**, pp. 115-123, 1983.

[3] Erhard A., Spindler K. and Hahne E., Test and simulation of a solar powered sorption cooling machine, *Int. J. Refrigeration*, **Vol. 21(2)**, pp. 133-141, 1998.

[4] Spinner B., Goetz V., Mazet N., Mauran S. and Stitou D., Performance of chemical reaction heat processes coupled to a solar source, *J. Phys. IV*, **Vol. 9**, pp. 355-360, 1999.

[5] Meunier F., Sorption solar cooling, *Renewable Energy*, **Vol. 5(1)**, pp. 422-429, 1994.

[6] Headley O.StC., Kothdiwala A.F. and McDoom I.A., Charcoal-methanol adsorption refrigerator powered by a compound parabolic concentrating solar collector, *Solar Energy*, **Vol. 53(2)**, pp. 191-197, 1994.

[7] Liu Z., Lu Y. and Zhao J., Zeolite-active carbon compound adsorbent and its use in adsorption solar cooling tube, *Solar Energy Materials and solar cells*, **Vol. 52**, pp. 45-53, 1998.

[8] Niemann M., Kreuzburg J., Schreitmüller K.R. and Leppers L., Solar process heat generation using an ETC collector field with external parabolic circle concentrator (PCC) to operate an adsorption refrigeration system, *Solar Energy*, **Vol. 59(1-3)**, pp. 67-73, 1997.

[9] Adell A., Description d'un réfrigérateur solaire à adsorption solide, étude de son fonctionnement en climat équatorial, *Rev. Gén. Therm. Fr.*, **Vol. 281**, pp. 529-536, 1985.

[10] Boubakri A., Arsalane M., Yous B., Ali-Moussa L., Pons M., Meunier F. and Guilleminot J.J., Experimental study of adsorptive solar-powered ice makers in Agadir (Morocco)-1. Performance in actual site, *Renewable Energy*, **Vol. 2 n°1**, pp. 7-13, 1992a.

[11] Boubakri A., Arsalane M., Yous B., Ali-Moussa L., Pons M., Meunier F. and Guilleminot J.J., Experimental study of adsorptive solar-powered ice makers in Agadir (Morocco)-2. Influences of meteorological parameters, *Renewable Energy*, **Vol. 2 n°1**, pp. 15-21, 1992b.

[12] Critoph R.E., An ammonia carbon solar refrigerator for vaccine cooling, *Renewable Energy*, **Vol. 5 part. I**, pp. 502-508, 1994.

[13] Critoph R.E., Tamainot-Telto Z. and Munyebvu E., Solar sorption refrigerator, *Renewable Energy*, **12(4)**, pp. 409-417, 1997.
[14] Grenier Ph., Guilleminot J.J., Meunier F. and Pons M., Solar powered solid adsorption cold store, *A.S.M.E. Trans.-J. Solar Energy Eng.*, **110**, 192-197, 1988.
[15] Marmottant B., Mhimid A., El Golli S. and Grenier Ph., Installation de réfrigération solaire à adsorption : expérimentation et modélisation, *Revue Gén. Thermique Fr.*, **362**, pp. 97-105, 1992.
[16] Mhiri F. and El Golli S., Etude d'un réfrigérateur solaire à adsorption solide avec le couple charbon actif-méthanol, *Rev. Gén. Therm.*, **Vol. 35**, pp. 269-277, 1996.
[17] Pons M. and Grenier Ph., Experimental data on a solar-powered ice maker using activated carbon and methanol adsorption pair, *J. Solar Energy Eng., ASME Trans.*, **Vol. 109**, pp. 303-310, 1987.
[18] Pons M. and Guilleminot J.J., Design of an experimental solar-powered, solid-adsorption ice maker, *J. Solar Energy Eng., ASME Trans.*, **Vol. 108**, pp. 332-337, 1986.
[19] Pralon Ferreira-Leite A. and Daguenet M., Performance of a new solid adsorption ice-maker with solar energy regeneration, *Energy Conversion and Management*, **Vol. 41**, pp. 1625-1647, 2000.
[20] Wang R.Z., Li M., Xu Y.X. and Wu J.Y., An energy efficient hybrid system of solar powered water heater and adsorption ice-maker, *Solar Energy*, **Vol. 68(2)**, pp. 189-195, 2000.
[21] Chassériaux J.M, *Conversion thermique du rayonnement solaire*, pp. 186-190, ISBN 2-04-015601-1,(1984).
[22] Howell J.R, Bannerot R.B, Vliet G.C, *Solar-Thermal Energy Systems, Analysis and Design*, pp. 122-129, ISBN 0-07-030603-6, (1982).

Nomenclature

COP	Coefficient of Performance	[-]
C_p	Specific heat	[J.kg^{-1}.K^{-1}]
G	Irradiance	[W.m^{-2}]
h	Heat transfer coefficient	[W.m^{-2}.K^{-1}]
L	Evaporation latent heat for water	[J.kg^{-1}]
m	Mass	[kg]
P	Pressure	[Pa]
Q	Heat quantity	[J]
S	Surface	[m^2]
t	Time	[s]
T	Temperature	[K]
ΔH	Desorption energy	[J.kg^{-1}]
ε	Adsorbed amount	[kg.kg^{-1}]
η	Collector efficiency	[-]
$(\tau\alpha)_{eff}$	Effective absorptance of cover-absorber	[-]

Indexes

a	ambient
A	beginning of heating (Figure 2)
C	cycle
c	condenser
coll	collector
cc	conductive transfer
cv	convective transfer
d	desorption
D	end of desorption (Figure 2)
e	evaporator
f	film Teflon
fs	collector front side
g	glass
h	solar heat supply
i	initial
j	tube section index
ls	collector lateral sides
L	liquid
N	nett
pa	Papyex®
R	rough
r	radiative transfer
ra	reflection - absorption
rs	collector rear side
S	solar
s	saturation
se	sensible
sg	silicagel
st	steel tube
t	tube
w	water